Korean J. Chem. Eng., **29**(2), 215-220 (2012)
DOI: 10.1007/s11814-011-0151-0

Bioactivity behaviour of biodegradable material comprising bioactive glass

Xuan Vuong Bui, Hassane Oudadesse†, Yann Le Gal, Odile Merdrignac-Conanec, and Guy Cathelineau

University of Rennes 1, UMR CNRS 6226, 263 av. Du Général Leclerc, 35042 Rennes Cedex, France
(*Received 7 April 2011 • accepted 7 June 2011*)

Abstract–Biocomposite of bioactive glass (BG) with chitosan polymer (CH) is prepared by freeze-drying technique. Obtained material is investigated by using several physico-chemical methods. The XRD and FTIR show the interface bonding interactions between glass and polymer. The specific surface and porosity of biocomposite were determined. *In vitro* assays were employed to evaluate the effect of chitosan addition on the glass by studying the chemical reactivity and bioactivity of the BG and BG/CH biocomposite after soaking in a simulated body fluid (SBF). The obtained results show the formation of a bioactive hydroxycarbonate apatite (HCA) layer and highlight the bioactivity and the kinetics of chemical reactivity of bioactive glass, particularly after association with chitosan. The BG/CH biocomposite has excellent ability to form an apatite layer. Inductively coupled plasma-optical emission spectrometry (ICP-OES) highlights the negative effect of chitosan on the silicon release toward the SBF of bioactive glass when *in vitro* assays.

Key words: Bioactive Glass, Biocomposite, "*In vitro*" Assays, Bioactivity, Freeze-drying

INTRODUCTION

Bioactive glasses are phosphosilicate glasses containing SiO_2-CaO-Na_2O-P_2O_5 networks. They are a group of osteoconductive biomaterials used as bone repair materials [1-4]. These materials are called bioactive because of the formation of interfacial bonds between the implant material and surrounding tissues. When these bioactive glasses are immersed in physiological solution or implanted in the human body, several serial reactions occur. Hench has described these reactions' following several steps: (1) rapid exchange of protons H_3O^+ from the physiological solution with Ca^{2+}, Na^+ ions in bioglass to form the Si-OH groups, (2) loss of soluble silica as $Si(OH)_4$ by breaking of Si-O-Si bridging links and subsequent formation of surface silanol groups in the process, (3) condensation and repolymerization of surface silanols to form SiO_2-rich surface layer, (4) migration of Ca^{2+} and PO_4^{3-} through the surface silica-rich layer and formation of a Ca-P rich layer on the surface of bioglass, (5) incorporation of OH^-, CO_3^{2-} from the solution and subsequent crystallization of the Ca-P layer to form an hydroxyl carbonate apatite layer (HCA). This apatite layer is similar to the inorganic component of human bone. It promotes the interface adhesion and the bonds between implant and natural bone. Consequently, the bone architecture is repaired and restored.

Chitosan is a natural biodegradable polymer. It is obtained by partial deacetylation of chitin, which is extracted from crustacean. Chitosan is currently the focus of medical research. It is considered as a suitable functional material for biomedical applications due to its good biocompatibility, biodegradability, non-antigenicity, anti-tumor activity, anti-inflammatory effect, protein adsorption properties and ability of accelerating wound healing [5-8]. Chitosan plays an important role in the attachment, differentiation and morphogenesis of osteoblasts, the bone forming cells, because of its structural similarities with glycosaminoglycans, a major component of bone and cartilage [9-10].

Composite materials of biodegradable polymers (as chitosan) and bioactive ceramics (as bioactive glass) have attracted much attention from material scientists because of their biological and physico-chemical advantages. The incorporation of bioactive glass particles into the chitosan polymer permit to obtain a porous structural material. They have an interconnected porous structure with the large enough sizes of pores to facilitate cell/tissue ingrowths [11-13]. Furthermore, the porous structure increases the surface area of biomaterials, which facilitates the contact between biomaterial and physiological solution; consequently, the bioactivity of the material can be enhanced. It is considered that the introduction of bioactive glass particles into chitosan polymer permits one to obtain an osteoinductive material, which has the capacity to induce regeneration or enhancement of functional bone.

The aim of this study is to incorporate both bioactive glass and chitosan polymer to obtain the bone-enhancing composite by using the freeze-drying technique. *In vitro* assays were carried out to highlight the effect of chitosan on the bioactivity and the kinetic of chemical reactivity of bioactive glass.

MATERIALS AND METHODS

1. Elaboration of Bioactive Glass/Chitosan Biocomposite

Bioactive glass (46S6) with composition $46SiO_2$-$24CaO$-$24Na_2O$-$6P_2O_5$ was elaborated by melting process [14]. Calcium silicate ($CaSiO_3$), sodium silicate (Na_2SiO_3) and sodium phosphate ($NaPO_3$) were weighted and mixed in a polyethylene bottle for 1 hour. The fusion of mixed powder was carried out in a platinum crucible at 1,300 °C during 3 hours. Afterward, the melted bioactive glass was poured into preheated brass moulds. The prepared samples were annealed at the glass transition temperature (about 536 °C) in a regu-

†To whom correspondence should be addressed.
E-mail: hassane.oudadesse@univ-rennes1.fr

lated muffle furnace, to remove the residual mechanical constraints. Then, they were cooled to room temperature. The bulk glasses were ground and sieved to obtain the bioactive glass particles with the particle size less than 40 μm.

To synthesize BG/CH biocomposite, the chitosan polymer with a medium molecular weight was dissolved in 1% acetic acid aqueous solution during 2 hours at room temperature to form a homogeneous viscous polymer solution. Then, the bioactive glass particles with the size less than 40 μm were suspended in chitosan solution. Mixture of bioactive glass particles and chitosan polymer was stirred during 2 hours at room temperature using magnetic stirring at 1,200 rpm (round per minute). After eliminating surplus solution, the mixture was frozen by liquid azotes and placed into a freeze-drying during 24 hours to totally exclude solvent. The obtained composite was immersed in 10% NaOH solution for two hours and washed several times with deionized water in order to neutralize the residues of acetic acid. Finally, the composite was frozen by liquid azotes and freeze-dried again for 24 hours to completely remove water. Biocomposite contained 17 wt% of chitosan polymer was synthesized according to the steps presented in Fig. 1.

2. In Vitro Assays in SBF Solution

Bioactivity and chemical reactivity of elaborated bioactive glass and biocomposite were investigated by soaking 30 mg of powdered samples into 60 ml of simulated body fluid (SBF) with pH and chemical composition similar to that of human blood plasma. The SBF solution was prepared using the method reported by Kokubo [15, 16]. Its ion concentrations are presented in Table 1. Powdered samples were immersed in SBF solution and maintained at body temperature (37 °C) under controlled agitation 50 rpm during 0, 1, 2, 3, 5, 7, 15 and 30 days. After soaking in SBF at different times, the powders were filtered, washed with deionized water to stop the reactions and then rinsed gently several times with absolute ethanol. Then, they were dried in an oven at 50 °C and stored to characterize the formation of apatite layer on their surfaces by using physico-chemical techniques.

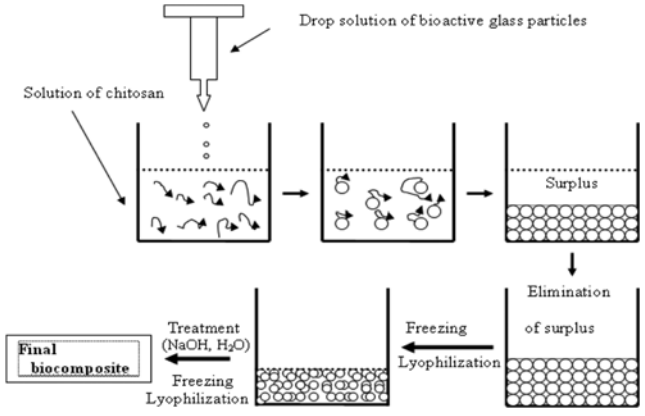

Fig. 1. Preparing protocols of biocomposite.

Table 1. Concentrations of the SBF solution, 10^{-3} mol·L^{-1}

Ions	Na^+	K^+	Ca^{2+}	Mg^{2+}	Cl^-	HCO_3^-	HPO_4^{2-}
SBF	142,0	5,0	2,5	1,5	148,8	4,2	1,0
Plasma	142,0	5,0	2,5	1,5	103,0	27,0	1,0

3. Instrumental Analysis Procedures

Several physico-chemical techniques were employed to characterize all powders before and after soaking in SBF. To characterize the chemical composition and crystallographic structure of synthetic materials and evaluate the formation of calcium phosphate layers, X-ray diffraction (XRD) measurements were realized on Philips PW 3710 diffractometer, using CuK_α radiation. Fourier transformed infrared absorption spectroscopy (FTIR) (Bruker Equinox 55) was used to identify the chemical links in the structure of biomaterials before soaking in SBF solution. It was also employed to refine the structure of apatite layer formed after *in vitro'* assays. The specific surface and porosity were determined by the N_2 adsorption-desorption measurements on multi point BET, ASAP 2010 Analyzer. The porosity percentage of biocomposite was determined using the liquid displacement method. Cyclohexane was used as the displacement liquid. The initial volume of cyclohexane was recorded as V_1. The biocomposite was immersed in this volume for 1 h. The obtained volume was recorded as V_2. The cyclohexane-impregnated biocomposite was removed and the residual cyclohexane volume was recorded as V_3. The (V_1-V_3) volume is the cyclohexane volume within the biocomposite. It is considered as the void volume of biocomposite. The (V_2-V_3) volume is the total volume of biocomposite. The percentage of porosity was determined by using the following relation: $[(V_1-V_3)/(V_2-V_3)]*100\%$. In addition, the inductively coupled plasma-optical emission spectrometry (ICP-OES) method which offers a high sensitivity less than 1 ppm was employed to evaluate the effect of chitosan on the dissolution of the glassy network versus soaking times by measurements of silicon released from biomaterials toward the synthetic physiological solution. Sample solution was nebulized (transformed into an aerosol) and carried by a gas carrier (usually Ar) through a torch, where a plasma (a gas in which atoms are ionized) was ignited. When sample atoms are ionized, they emit radiation at some specific wavelength. These specific components were selected by a diffracting grating, and converted in electric signals by a photomultiplier. After calibration, it is possible to determine the amount of each element present in solution by analyzing the intensity of the radiation emitted at the specific elemental frequency.

RESULTS AND DISCUSSIONS

1. Physico-chemical Characterizations

1-1. Specific Surface and Porosity

Fig. 2 shows the graphical form of the BET isothermal line. It exhibits a type IV isotherm, typical of a mesoporous structure. The data of the specific surface area, of pore volume and pore size are listed in Table 2. The specific surface areas of bioactive glass and chitosan are 0.90 and 0.70 (m^2/g), respectively, while the specific surface area of biocomposite is 14.9 (m^2/g). Thus, the specific surface area of biocomposite is more than sixteen- and twenty-one times, respectively, in comparison with bioactive glass and chitosan polymer. In addition, the percentage of porosity of biocomposite is determined by the liquid displacement method. This experimental value is 80%. These obtained results highlight the large specific surface area and the high void ratio of biocomposite in comparison with bioactive glass and chitosan polymer.

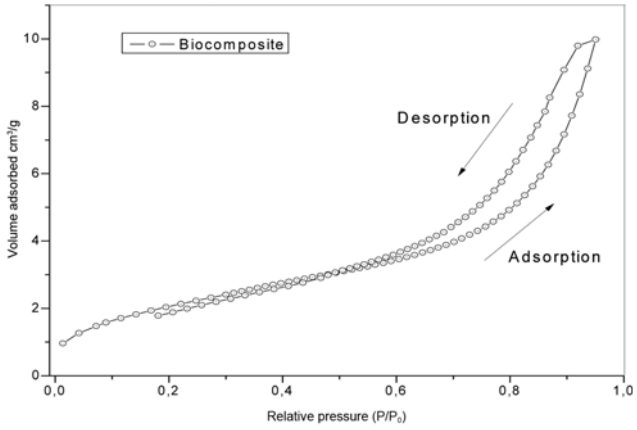

Fig. 2. N_2 adsorption-desorption isotherm line of biocomposite.

Table 2. Specific surface area and porosity

Samples	S_{BET} (m^2/g)	Pore volume (m^3/g)	Pore diameter (nm)	Void ratio (%)
Bioactive glass	0.9	-	-	-
Chitosan	0.7	-	-	-
Biocomposite	14.9	0.015	8	80

As references, Sepulveda reported that the melt-derived bioglass 45S5 powders exhibited a low-porosity texture with surface area in the range 0.15-2.7 (m^2/g) [17]. In another work, Bumgardner presented the elaboration of chitosan/hydroxyapatite composite microsphere which possessed a limited value of specific surface area (0.707 m^2/g) [12]. These data highlight the success on the aspect of specific surface area of our biocomposite.

1-2. XRD Analysis

The XRD diagrams of bioactive glass, chitosan polymer and biocomposite before *in vitro* assay are shown in Fig. 3. The XRD diagram of bioactive glass did not show any evidence of crystalline phase and confirmed the amorphous character of glass. It presents a diffraction halo between 20 and 40° (2θ) with center at 32.5°. This diffraction halo is characteristic of the diffusion phenomena in amorphous materials and the absence of long range order in the matrix of bioactive glass. It consists of an amorphous material. The chitosan polymer presents one characteristic peak at about 20° (2θ). It corresponds to type II orthorhombic crystallization of chitosan [18]. The XRD diagram of biocomposite presents the characteristic amorphous nature of bioactive glass. It also illustrates the presence of chitosan polymer. In detail, the characteristic peak of chitosan polymer at 20° is shown. The center of diffraction halo characterized to bioactive glass at 32.5° is found but it is shifted to the left. One new peak at 29° occurs. The shift and appearance of new peaks observed in diffraction diagram of biocomposite highlight the chemical interactions between bioactive glass and chitosan polymer which induce the changes in amorphous structure of glass.

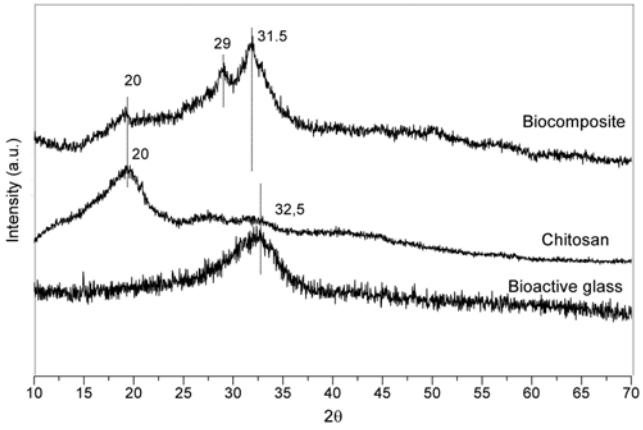

Fig. 3. XRD diagrams of Bioactive glass, Chitosan and biocomposite.

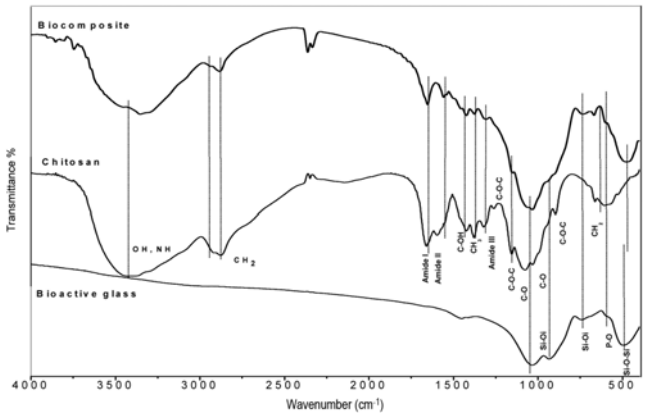

Fig. 4. IR spectra of Bioactive glass, Chitosan and biocomposite.

1-3. FTIR Analysis

Fig. 4 presents the IR spectra of bioactive glass, of chitosan and of biocomposite. The IR spectrum of bioactive glass shows several characteristic bands of silica network. The band at 503 cm^{-1} is attributed to an angular deformation vibration of Si-O-Si between SiO_4 tetrahedrons. Three other bands at 745, 932 and 1,036 cm^{-1} respectively are characteristic of stretching vibration of Si-O chemical bond in SiO_4 tetrahedron. The last band at 590 cm^{-1} is characteristic of bending vibration of O-P-O liaison. Its slight intensity highlights the presence of a small amount of phosphate linked to the vitreous matrix [19-22].

The IR spectrum of chitosan polymer shows absorption band at 3,000-4,000 cm^{-1} for stretching vibration of -NH_2 and -OH groups. On the other hand, the characteristic bands at 1,657, 1,597 and 1,320 cm^{-1} are assigned to the amide one, amide two and amide three absorption bands, respectively. The methylene (-CH_2-) groups are characterized by the bands at 2,926, 2,880 and 665 cm^{-1}. The characteristic band at 1,380 cm^{-1} is characteristic of stretching vibration of methyl (-CH_3) groups due to incomplete deacetylation of the parent chitin in the synthesis of chitosan polymer. The band at 1,422 cm^{-1} is characteristic of bending vibration of C-OH group. The bands at around 1,075 and 1,033 cm^{-1} are attributed to C-O stretching vibrations in the chitosan skeletal. Two absorption bands at 1,153 and 890 cm^{-1} are characteristic of stretching vibrations of C-O-C groups in saccharide structure of chitosan [23-28].

Several characteristic bands of chitosan polymer and of bioactive glass are shifted, disappeared or deformed after biocomposite formation. That highlights the chemical interactions between bio-

active glass and chitosan polymer. For the chitosan polymer, the characteristic band of amide II group is shifted to the short wave while the band of amide III group is shown with a slight intensity. The characteristic bands of bridging C-O-C groups and C-O groups in chitosan skeleton are exhibited with slight intensity or disappeared. For the bioactive glass, two characteristic bands at 932 and 1,036 cm^{-1} (Si-O) present an important distortion. The characteristic band at 503 cm^{-1} (Si-O-Si) is shifted to a short wave. The above changes of characteristic bands illustrate the participation in bonding of both bioactive glass and chitosan polymer after biocomposite formation.

2. Physico-chemical Reactions of Biomaterials after *In Vitro* Assays

2-1. XRD Structural Analysis of Bioactive Apatite Layer

X-ray diffraction (XRD) is used to clarify the precipitation of mineral apatite on the surface of bioactive glass and of biocomposite after soaking in SBF solution. Figs. 5-6 present the XRD diagrams of bioactive glass and of biocomposite, respectively, after 3 and 15 days soaking in SBF solution. The XRD diagram of hydroxyapatite is presented as reference for comparison with these materials [29,30]. After soaking in SBF solution, the initial structures of these two biomaterials are modified strongly due to the interfacial reactions between the biomaterials and the physiological solution. The hydroxyapatite formation is witness to illustrate the bioactivity of bioactive glass and biocomposite.

After three days of soaking in SBF, the immersed bioactive glass is still amorphous material and the characteristic peaks of hydroxyapatite can't be observed on its XRD diagram. However, five peaks at 26°, 32°, 40°, 50° and 53° appear in the XRD diagram of biocomposite. They correspond, respectively, to the (002), (211), (310), (213) and (004) plane reflections of hydroxyapatite crystals. The obtained result highlights the rapid formation of apatite layer on the surface of biocomposite induced by the presence of chitosan polymer. The presence of chitosan in the glassy matrix accelerates the interactions and ionic exchanges between biocomposite and environment medium. That leads to the rapid formation of apatite layer.

After 15 days of soaking in SBF solution, the XRD diagram of bioactive glass shows five characteristic peaks of hydroxyapatite layer at 26° (002), 32° (211), 40° (310), 50° (213) and 53° (004). The XRD diagram of biocomposite shows seven peaks at 26° (002), 32° (211), 40° (310), 46.7° (222), 50° (213), 53° (004) and 64° (304). It is recognized that the hydroxyapatite peaks formed on the surface of biocomposite are more visible than the one of bioactive glass. That highlights the good crystallization of apatite layer on the surface of biocomposite. The presence of chitosan is also responsible for the crystallization quality of formed apatite layer.

In summary, the kinetic and quality of hydroxyapatite layer formation on the surface of biocomposite is faster than the one of pure bioactive glass. As soon as three days of soaking in SBF solution, it presents already the characteristic peaks of hydroxyapatite layer. After 15 days, it shows all characteristic peaks of hydroxyapatite layer. This result is important because it permits the use of this biocomposite in bony surgery when the bony metabolism presents a high activity in young patients, for example.

2-2. FTIR Structural Analysis of Bioactive Apatite Layer

The FTIR spectra of bioactive glass and of biocomposite after 3 days and 15 days of soaking in SBF solution are shown in Figs. 7-8. The IR spectrum of synthetic hydroxyapatite is used as reference to evaluate the interactions and links created in prepared biomaterials [29]. After soaking in SBF solution, the structure of bioactive glass and biocomposite is changed due to the interfacial chemical reactions between these biomaterials and the physiological solution, which leads to the formation of apatite layer.

In detail, the IR spectrum of biocomposite reveals three new well-

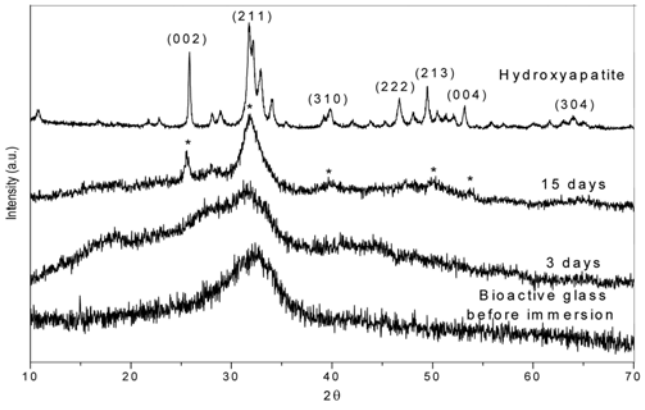

Fig. 5. XRD diagrams of Bioactive glass after soaking 3 and 15 days in SBF solution and hydroxyapatite.

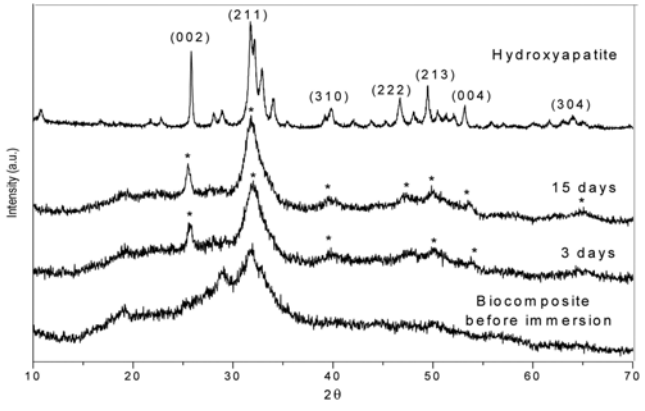

Fig. 6. XRD diagrams of Biocomposite after soaking 3 and 15 days in SBF solution and hydroxyapatite.

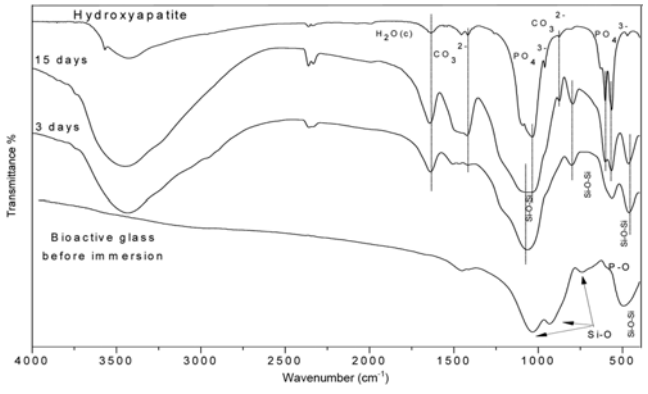

Fig. 7. IR spectra of Bioactive glass after 3 and 15 days of soaking in SBF solution and hydroxyapatite.

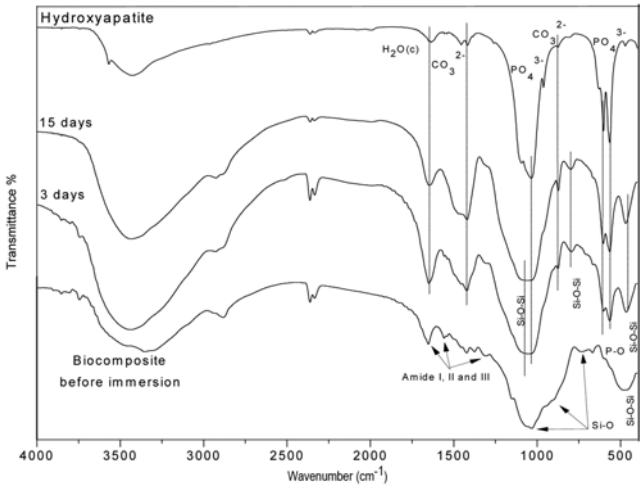

Fig. 8. IR spectra of Biocomposite after 3 and 15 days of soaking in SBF solution and hydroxyapatite.

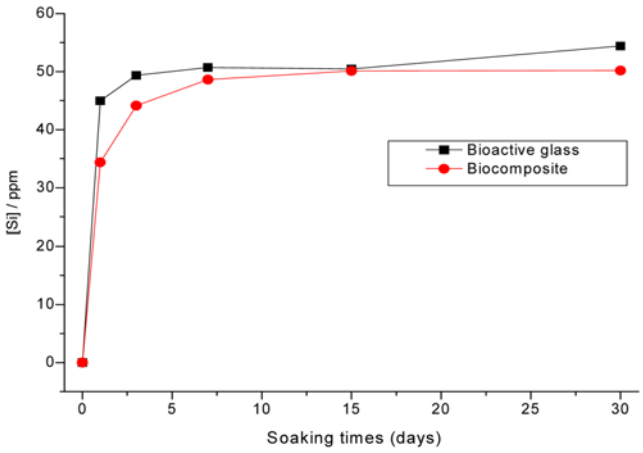

Fig. 9. Evolution of Si concentrations in SBF solution measured by ICP-OES, versus soaking times.

defined phosphate bands at 565, 603 and 1,039 cm^{-1} after three days of soaking in physiological solution. They are assigned to stretching vibrations of PO_4^{3-} group in phosphate crystalline phases. Simultaneously, the carbonate bands at 874 and 1,420 cm^{-1} are also observed. They are characteristic of C-O bending vibration and C-O stretching vibration respectively in carbonate groups. These results confirm the formation of a bone-like carbonated hydroxyapatite layer on the surface of biocomposite after soaking in SBF. After three days of soaking in SBF solution, the IR spectrum of bioactive glass does not present the characteristic bands of apatite layer. The obtained results highlight the rapid formation of apatite layer on the surface of biocomposite.

After 15 days of soaking in SBF solution, the IR spectrum of bioactive glass exhibits the characteristic bands of carbonated hydroxyapatite layer. Three bands at 565, 603, 1,039 cm^{-1} are characteristic of PO_4^{3-} groups. Two bands at 874, 1,420 cm^{-1} correspond to CO_3^{2-} groups. It is recognized that the characteristic bands observed on the IR spectrum of biocomposite are more visible than the one of bioactive glass. That confirms the high quality of apatite crystallization on the surface of biocomposite.

In addition, the IR spectra of glass and biocomposite also exhibit three Si-O-Si bands at 470 cm^{-1} (bending vibration), 799 cm^{-1} (bending vibration) and 1,075 cm^{-1} (stretch vibration) after 3 and also 15 days of soaking in physiological solution. These bands are characteristic of pure silica. This result confirms the formation of a SiO_2 gel on the surface of glass and biocomposite after *in vitro* assays. Thus, the silica gel is formed before the apatite layer. These results are in accordance with the mechanism of the physico-chemical interactions bioglasses/physiological solution invented by Hench which is presented in the introduction part.

These obtained results are totally in accordance with the analyses obtained by XRD. They highlight the positive effect of chitosan polymer on the bioactivity of bioactive glass. The biocomposite-based bioactive glass and chitosan polymer shows a rapid formation of well crystallized apatite layer on its surface and in a short time in comparison with initial bioactive glass.

2-3. ICP-OES Investigation of Silicon Release from the Glassy Network

Fig. 9 presents the variations of Si concentrations, measured by ICP-OES method. The release of silicon toward the simulated body fluid (SBF) is coherent with the dissolution of glassy network. The bioactive glass presents an important release after the first days of immersion in SBF. The silicon concentration in SBF increases very strong from 0 ppm to 45 ppm. Then, it increases an amount of about 5 ppm after three days of soaking. After that, there is no significant modification of silicon concentration.

The presence of chitosane in biocomposite delays the silicon release toward the synthetic physiological liquid. The silicon ions concentration increases strongly during the first day of immersion. Then, it increases slowly till seven days of soaking. After seven days of immersion, the silicon ion concentration is almost saturated. The silicon ion amount released from biocomposite is always lower than the one of bioactive glass. It is considered that the chitosan polymer acts as a capping agent to delay the silicon release from glassy network.

CONCLUSION

Bone-enhancing biocomposite of bioactive glass and chitosan synthesized by freeze - drying technique are very promising. The obtained biocomposite is investigated by several physico-chemical methods. The XRD and FTIR show the interface bonding interactions between glass and polymer. The "*in vitro*" assays are realized for both bioactive glass and biocomposite by soaking of powdered samples in SBF solution. The obtained results confirm the formation of hydroxyapatite layer on their surfaces and highlight the effects of chitosan addition. First, the chitosan polymer delays the silicon release from glassy network. Second, the presence of chitosan enhances the bioactivity of bioactive glass. The biocomposite based on bioactive glass and chitosan polymer shows an excellent capacity to form a hydroxyapatite layer on its surface. After three days of soaking in SBF, the analyses by XRD confirm the formation of this layer. It is considered that the porosity of biocomposite is the basic reason of excellent capacity to form the hydroxyapatite. The porosity facilitates contact between the biocomposite and the simulated body fluid. Thus, the ionic exchanges between the biocomposite and the SBF became easy. That improves the bioactivity of

biomaterials. More, the effects of chitosan polymer could be weakening the links in the vitreous matrix of bioactive glass. This favors the breaking of links in the glassy network under the SBF solution effect. Consequently, the surface reactions between the biocomposite and the physiological solution became rapid. That leads to fast the formation of apatite layer. The advantages of these two bioactivity kinetics consist in their adaptation for different cases in their application in the biomaterial field. The bioconsolidation in the interface biomaterial/bone depends widely on the age, gender, location site and bony metabolism. Concerning the young body where the metabolism activities are very intense, it would be suitable to use the biocomposite because of rapid formation of hydroxyapatite layer on the surface; this one is responsible for a good bioconsolidation. The bioactive glass/chitosan biocomposite synthesized from bioactive glass particles and chitosan polymer using the freeze-drying technique is promising in terms of its bioactivity, and may find potential applications in the biomedical domain.

REFERENCES

1. L. L. Hench, R. J. Splinter, W. C. Allen and T. K. Greenlee, *J. Biomed. Mater. Res.*, **5**, 117 (1971).
2. H. Oudadesse, M. Mami, R. Doebez-Sridi, P. Pellen, F. Perez, S. Jeanne, D. Chauvel-Lebret, A. Mostafa and G. Cathelineau, *Biocer-amics*, **22**, 379 (2009).
3. L. L. Hench, *J. Mater. Sci.: Mater. Med.*, **17**, 967 (2006).
4. L. L. Hench and J. K. West, *Life Chem. Rep.*, **13**, 187 (1996).
5. G. Brandenberg, L. G. Leibrock, R. Shuman, W. G. Malette and H. Quigley, *Neurosurgery*, **15**, 9 (1984).
6. R. A. Muzzarelli, F. Tanfani, M. Emanuelli, D. P. Pace and E. Chiumzzi, *Carbohydr. Res.*, **126**, 225 (1984).
7. S. Hirano and Y. Yagi, *Carbohydrates*, **8**, 103 (1980).
8. L. Jiang, Y. Li, X. Wang, L. Zhang, J. Wen and M. Gong, *Carbohydr. Polym.*, **74**, 680 (2008).
9. M. Peter, N. S. Binulal, S. Soumya, S. V. Nair, T. Furuike, H. Tamura and R. Jayakumar, *Carbohydr. Polym.* (2009).
10. R. A. Muzzarelli, *Carbohydr. Polym.*, **83**, 1433 (2011).
11. B. D. Boyan, G. Niederauer, K. Kieswetter, N. C. Leatherbury and D. C. Greenspan, United States Patent (1999).
12. J. D. Bumgardner, B. M. Chesnutt, W. O. Haggard, Y. Yuan, T. M. Utturkar and B. Rever, United States Patent (2007).
13. M. Peter, N. S. Binulal, S. V. Nair, N. Selvamurugan, H. Tamura and R. Jayakumar, *Chem. Eng. J.*, **158**, 353 (2010).
14. E. Dietrich, H. Oudadesse, A. Lucas-Girot and M. Mami, *J. Biomed. Mater. Res.*, **88A**, 1087 (2008).
15. T. Kokubo, H. Kushitani, S. Sakka, T. Kitsugi and T. Yamamuro, *J. Biomed. Mater. Res.*, **24**, 721 (1990).
16. T. Kokubo and H. Takadama, *Biomaterials*, **27**, 2907 (2006).
17. S. Sepulveda, J. R. Jones and L. L. Hench, *J. Biomed. Mater. Res.*, **58**, 734 (2001).
18. Z. Zong, Y. Kimura, M. Takahashi and H. Yamane, *J. Polym.*, **41**, 899 (2000).
19. I. Lebecq, Thèse, Université de Valenciennes (2002).
20. M. Sitarz, W. Mozgawa and M. Handke, *J. Mol. Structure*, **511**, 282 (1999).
21. M. Handke, M. Sitarz, M. Rokita and E. Galuskin, *J. Mol. Structure*, 651 (2003).
22. S. A. MacDonald, C. R. Schardt, D. J. Masiello and J. H. Simmons, *J. Non-Crystalline Solids*, 275 (2000).
23. M. Guiping, Y. Dongzhi, J. F. Kennedy and N. Jun, *Carbohydr. Polym.*, **75**, 390 (2009).
24. M. Guiping, Y. Dongzhi, Z. Yingshan, X. Ming, J. F. Kennedy and J. Nie, *Carbohydr. Polym.*, **74**, 121 (2008).
25. H. Y. Kweon, I. C. Um and Y. H. Park, *Polymer*, **42**, 6651 (2001).
26. J. Wang, C. Liu, J. Wei, P. Chi, X. Lu and M. Yin, *Biomed. Mater.*, **2**, 32 (2007).
27. Y. Baimark, P. Srihanam and Y. Srisuwan, *Current Res. Chem.*, **1**, 8 (2009).
28. X. D. Liu, S. Tokura, N. Nishi and N. Sakairi, *J. Polym.*, **44**, 1021 (2003).
29. P. Luo, United States Patent (1999).
30. Fiche JCPDF 09-432.